AD-A097 722 NAVAL OCEAN SYSTEMS CENTER SAN DIEGO CA F/G 9/1
PERFORMANCE OF LIGHT-EMITTING DIODES UNDER HYDROSTATIC PRESSURE--ETC(U)
JAN 81 G A GARCIA
UNCLASSIFIED NOSC-TR-651 NL

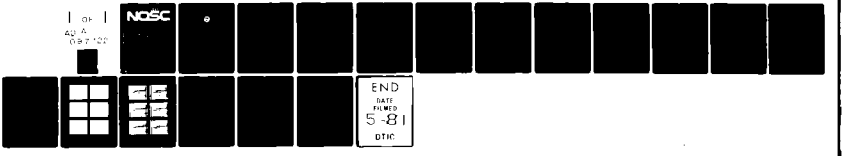

LEVEL II

12

NOSC

NOSC TR 651

NOSC TR 651

Technical Report 651

PERFORMANCE OF LIGHT-EMITTING DIODES UNDER HYDROSTATIC PRESSURE

GA Garcia

January 1981

Final Report: May - September 1980

Prepared for
Naval Underwater Systems Center

Approved for public release; distribution unlimited.

NAVAL OCEAN SYSTEMS CENTER
SAN DIEGO, CALIFORNIA 92152

NAVAL OCEAN SYSTEMS CENTER, SAN DIEGO, CA 92152

AN ACTIVITY OF THE NAVAL MATERIAL COMMAND

SL GUILLE, CAPT, USN
Commander

HL BLOOD
Technical Director

ADMINISTRATIVE INFORMATION

The work reported herein was conducted for the Naval Underwater Systems Center over the period May–September 1980 under Program Element 62543N, Task XF43453401.

Released by
IP Lemaire, Head
Advanced Systems Division

Under authority of
HR Talkington, Head
Ocean Technology Department

UNCLASSIFIED

SECURITY CLASSIFICATION OF THIS PAGE (When Data Entered)

REPORT DOCUMENTATION PAGE

READ INSTRUCTIONS BEFORE COMPLETING FORM

1. REPORT NUMBER: NOSC Technical Report 651 (TR 651)

2. GOVT ACCESSION NO.: AD-A097 422

3. RECIPIENT'S CATALOG NUMBER:

4. TITLE (and Subtitle): PERFORMANCE OF LIGHT-EMITTING DIODES UNDER HYDROSTATIC PRESSURE

5. TYPE OF REPORT & PERIOD COVERED: Final report, May - Sep[illegible]1980

6. PERFORMING ORG. REPORT NUMBER:

7. AUTHOR(s): G.A. Garcia

8. CONTRACT OR GRANT NUMBER(s): 62543N, XF43453401

9. PERFORMING ORGANIZATION NAME AND ADDRESS: Naval Ocean Systems Center, San Diego, CA 92152

10. PROGRAM ELEMENT, PROJECT, TASK AREA & WORK UNIT NUMBERS:

11. CONTROLLING OFFICE NAME AND ADDRESS: Naval Underwater Systems Center, New London, CT

12. REPORT DATE: Jan[illegible]1981

13. NUMBER OF PAGES: 15

14. MONITORING AGENCY NAME & ADDRESS (if different from Controlling Office): NOSC/TR-651

15. SECURITY CLASS. (of this report): Unclassified

15a. DECLASSIFICATION/DOWNGRADING SCHEDULE:

16. DISTRIBUTION STATEMENT (of this Report)

Approved for public release; distribution unlimited.

17. DISTRIBUTION STATEMENT (of the abstract entered in Block 20, if different from Report)

18. SUPPLEMENTARY NOTES

19. KEY WORDS (Continue on reverse side if necessary and identify by block number)
electro-optics
underwater sensors
GaA/As diodes
Pressure-tolerant electronics

20. ABSTRACT (Continue on reverse side if necessary and identify by block number)

The effect of hydrostatic pressure on two types of light-emitting diodes is presented. Emission characteristics and source-to-optical-fiber coupling performance were examined under conditions which simulate those found in a fluid-filled, pressure-equalizing enclosure. Minimal changes in either emission or coupling characteristics were observed at pressures up to 10 000 psi.

DD FORM 1 JAN 73 1473 EDITION OF 1 NOV 65 IS OBSOLETE
S/N 0102-LF-014-6601

UNCLASSIFIED 393159

SECURITY CLASSIFICATION OF THIS PAGE (When Data Entered)

CONTENTS

ILLUSTRATIONS

INTRODUCTION

The undersea environment places special demands on the design of electro-optic and fiber-optic systems. Isolation of the optical system from the rigors of the deep ocean through encapsulation in hermetically sealed pressure containers is one solution to the problems faced by the electro-optical engineer who is interested in sub-surface deployment. An alternative approach which avoids the bulk and inconvenience of pressure containers and associated pressure hull penetrators is to design the electro-optic system to perform satisfactorily in a fluid-filled, pressure-equalized package which subjects the components to the ambient pressure encountered at depth.

At the heart of any fiber-optic system are the light source and the source-to-fiber coupling arrangement. This report focuses on these components, with the primary emphasis placed on the hydrostatic pressure behavior of the source and source–fiber interface. Two types of LED sources were studied: the Spectronics SE0352 surface emitter and the RCA C30123 edge emitter. Figures 1 and 2 show the coupling geometry used for the surface and edge emitters, respectively. Both sources were coupled to step-index optical fiber having the following specifications:

core diameter	100 μm
outside diameter	140 μm
numerical aperture (N.A.)	0.3

Several characteristics of the source and the source–fiber interface were examined under conditions which simulate those found in a fluid-filled, pressure-equalized enclosure. Optical coupling efficiency, defined to be the ratio of power coupled into the fiber core to the total power emitted by the source, was measured in air and compared to data obtained in a mineral oil ambient. Immersion in a high-index medium such as mineral oil ($n \approx 1.50$) was expected to change the coupling efficiency by altering the effective N.A. of the fiber and the emission characteristics of the LED. Potential changes in the output rise and fall times of the LEDs due to pressure-induced effects on the fundamental material properties of GaAlAs were also investigated. Lastly, the emission spectra of the two LEDs were recorded at pressure to determine whether lattice compression would significantly affect the distribution of light power vs wavelength.

TEST APPARATUS AND PROCEDURES

Hydrostatic pressures from 0 to 10000 psi were obtained with a conventional hand-actuated piston and check-valve pump which forced mineral oil into a pressure vessel equipped with electrical penetrators. Optical signals were transmitted out of the pressure vessel through a pressure-bearing window in the upper end closure. Hydraulic oil temperature was measured as a function of oil pressure under simulated LED test conditions using a thermocouple situated near the center of the pressure vessel interior. The temperature could not be monitored during the course of the optical measurements due to a limited number of electrical penetrators.

Measurements of the optical power coupled into the fiber core were obtained with a PIN photodiode attached to the cleaved fiber end. LED forward current (DC) and coupled PIN photocurrent passed through the pressure vessel by way of penetrators in the lower end closure. A 3-cm section of the fiber was stripped and coated with black paint in order to extinguish power in the fiber cladding modes.

Output rise and fall times were determined with the aid of a pressure-tolerant driver circuit which resided in the pressure vessel. An internally located driver circuit avoided the impedance irregularity encountered at the pressure vessel electrical penetrators, which may have hampered attempts at measuring short rise times. This circuit (Figure 3) consisted of an ECL multivibrator followed by a three-stage amplifier, all the components of which were selected for their insensitivity to hydrostatic pressure. The drive signal was a 50-percent-duty-cycle 1-MHz square wave which delivered 200 mA of forward current with rise and fall times of approximately 1 ns. Optical power from the cleaved fiber end was collimated with a 1/4-pitch, graded-index rod lens, transmitted through the glass window in the end closure, and focused onto a high-speed photodetector mounted outside of the pressure vessel (Figure 4). Detection of the output signal was achieved with a PIN diode followed by a transimpedance amplifier whose bandwidth limited the photodetection rise time to about 3 ns. A Tektronix 485 oscilloscope having a 1-ns rise time was used to record the rising and falling edges.

Spectral information was gathered using a grating monochromator to analyze the optical signal emanating from the pressure vessel. A 1-kHz square wave drove the LED to forward current levels of 150 mA, and the resulting optical pulses were collimated, passed through the pressure vessel window, and focused onto the monochromator entrance slits. The output signal from the monochromator was detected synchronously by means of a lock-in amplifier tuned to the 1-kHz LED drive signal.

RESULTS

COUPLED POWER

According to Gilbert*, immersion in a high-index medium, as compared to air, should significantly increase the coupling efficiency of an edge-emitting LED. Our measurements indicate, however, only a 1-dB change in coupled power for the RCA C30123 edge emitter when this device is immersed in mineral oil. Gilbert predicts a 2.7-dB increase in coupling efficiency for edge emitters in silicone oil ($n = 1.48$). It should be noted, however, that Gilbert's calculation assumes a flat, perpendicular fiber endface. Since our measurements were made with a lensed fiber end, one may expect a smaller increase in coupling efficiency following oil immersion, although this hypothesis has not been checked in detail. The surface emitter showed a much smaller increase in coupling efficiency, about 0.35 dB in an oil ambient, than the edge emitter.

Application of hydrostatic pressure affected the coupling efficiency of the surface emitter to an immeasurably small extent. Figure 5 shows a plot of the coupled power, with constant forward current, for the Spectronics SE0352 surface emitter at pressures up to 10 000 psi. Data gathered preceding and following 10 pressure cycles to 2 000 psi showed constant coupling efficiency for all pressures of interest. Figure 6 reveals somewhat different pressure behavior for the edge emitter. Before pressure cycling, the coupling efficiency decreased by about 1.2 dB from 0 to 10 000 psi. Following 10 pressure cycles to 2 000 psi,

* DF Gilbert, FF Manes, and FC Allard, Conference Record, Oceans '80.

the pig-tailed edge emitter stabilized and showed only an 0.4-dB decrease in coupling efficiency while undergoing a pressure increase of 10 000 psi. This behavior is probably due to small voids in the epoxy bond between the fiber and the V-block which compress and perturb the LED-to-fiber alignment. Pressure cycling causes the epoxy to settle into a more pressure-insensitive configuration, which maintains the LED-to-fiber relationship.

RISE AND FALL TIME

Oscilloscope traces of the amplified photodetector outputs are shown in Figures 7 and 8. For both LED types, the rise time was found to be within the manufacturers' specifications for the entire pressure range from 0 to 10 000 psi. In fact, no change in the LED rise time with increasing pressure could be discerned for either LED. Interestingly, the fall times for both LED types were found to be shorter than the rise times. Again, no pressure-induced changes in the fall time could be detected. Higher pressures are apparently needed in order to produce measurable changes in intrinsic device characteristics, such as junction capacitance and recombination lifetime, which determine LED rise and fall times.

SPECTRAL DISTRIBUTION

Figures 9 and 10 are plots of the optical output power as a function of wavelength for both LEDs at 0 and 10 000 psi. A small but measurable shift in the spectral distribution can be seen. In both cases, the shift is of the order of 20–30 Å towards shorter wavelengths and can be attributed to a pressure-induced increase in the radiative bandgap of GaAlAs.

TEMPERATURE

For reference, the temperature of the hydraulic oil is shown in Figure 11 as a function of oil pressure. Within the error of the measurement, which was determined primarily by fluctuations in the thermocouple reference temperature, the oil temperature remained constant over the pressure range of interest.

CONCLUSIONS

Hydrostatic pressure of the magnitude encountered in any conceivable undersea application is not likely to degrade the performance of either of the LED types studied here. In fact, the purely optical effects of the oil medium on the characteristics of the LED and the LED-fiber interface are usually greater than the effects attributable to hydrostatic pressure. Emphasis should, therefore, be placed on selecting a pressure-equalizing fluid which does not adversely interact either chemically or optically with the electro-optic system.

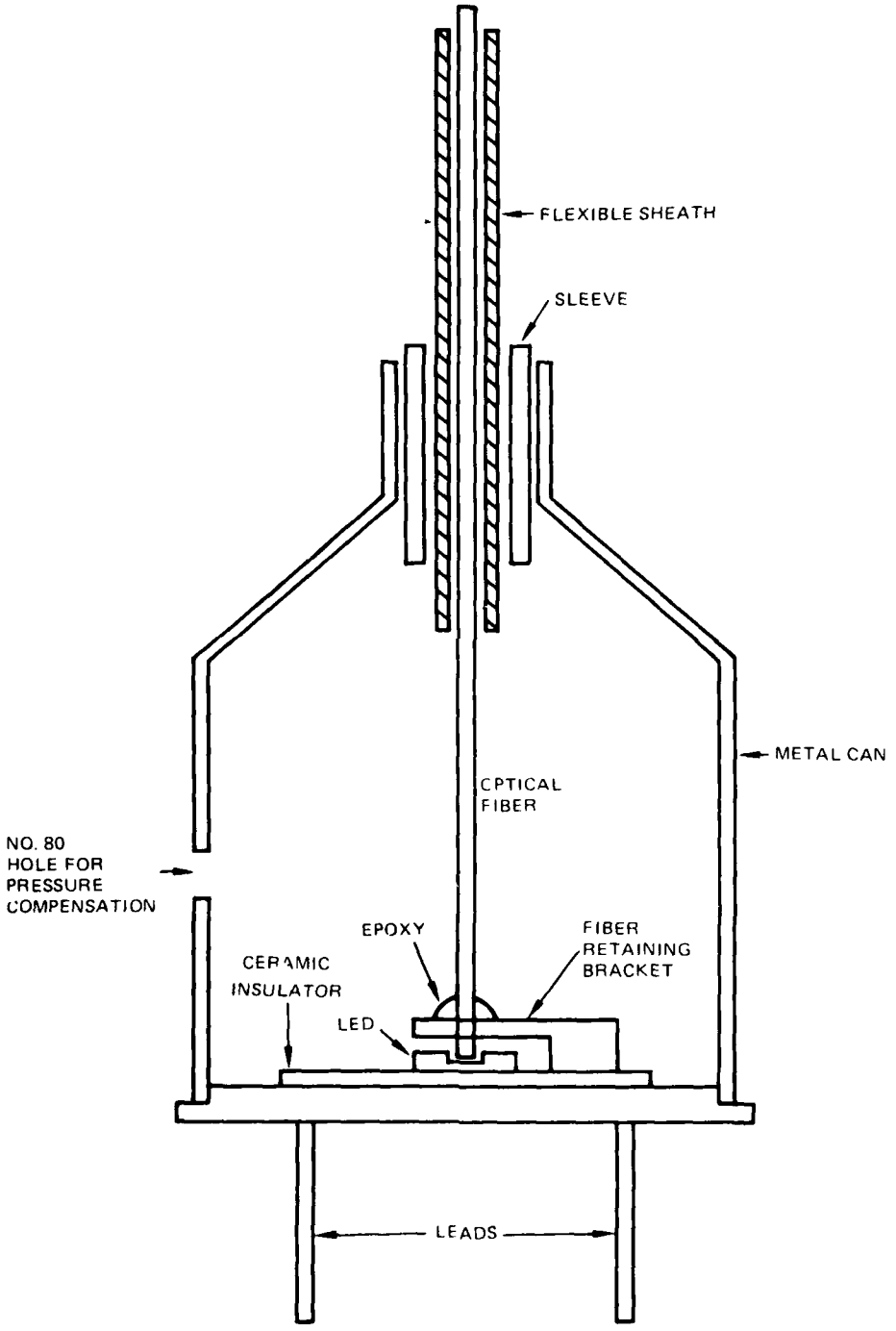

Figure 1. Coupling geometry for the Spectronics SE0352 surface emitter

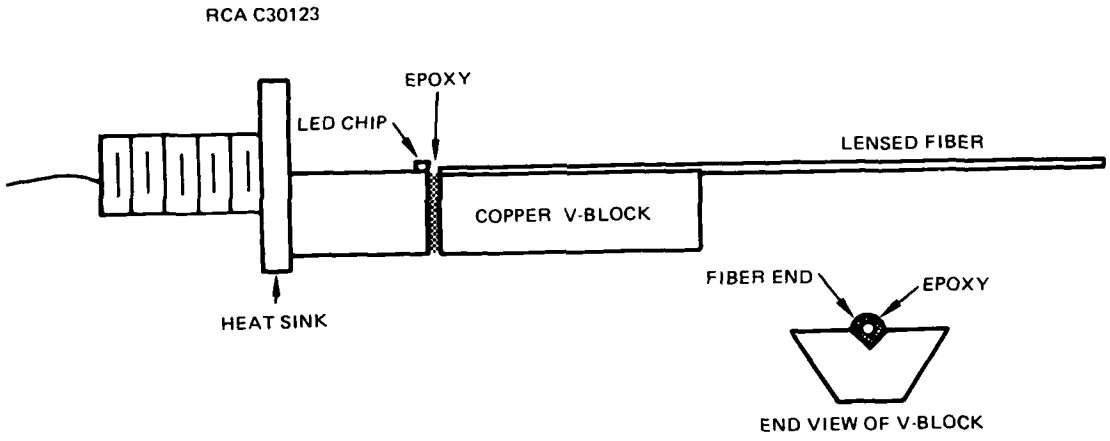

Figure 2. Coupling geometry for the RCA C30123 edge emitter.

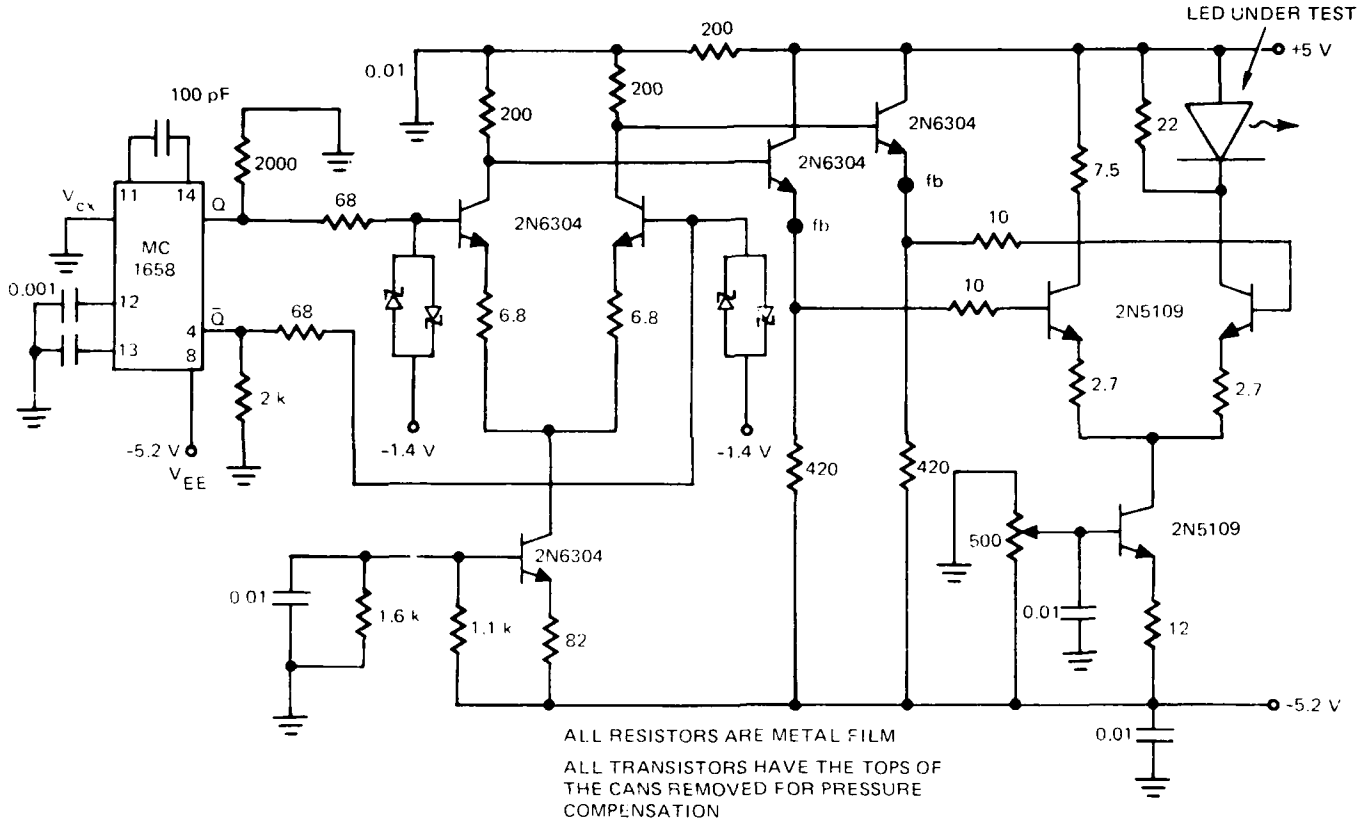

Figure 3. LED rise time test circuit

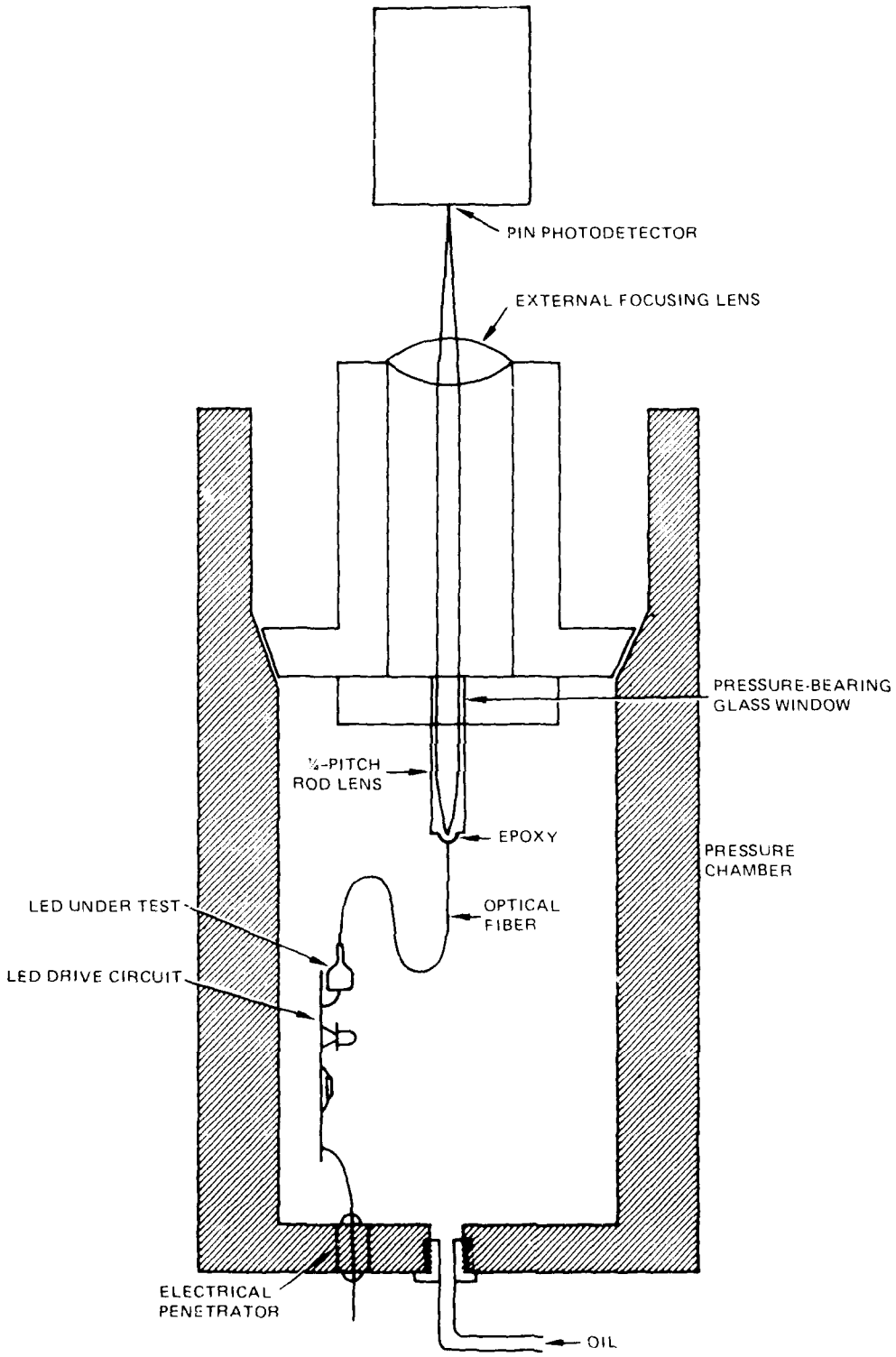

Figure 4. Apparatus for measurement of LED rise time at pressure.

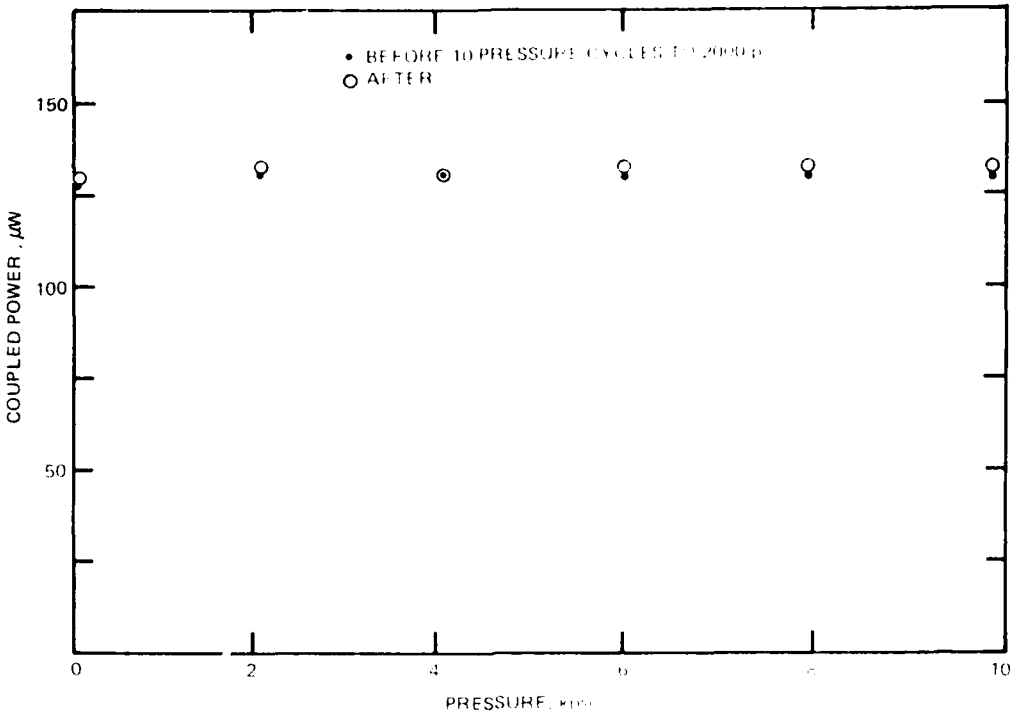

SPECTRONICS SE0352 80 mA FORWARD CURRENT

Figure 5. Coupled power vs pressure for the Spectronics SE0352.

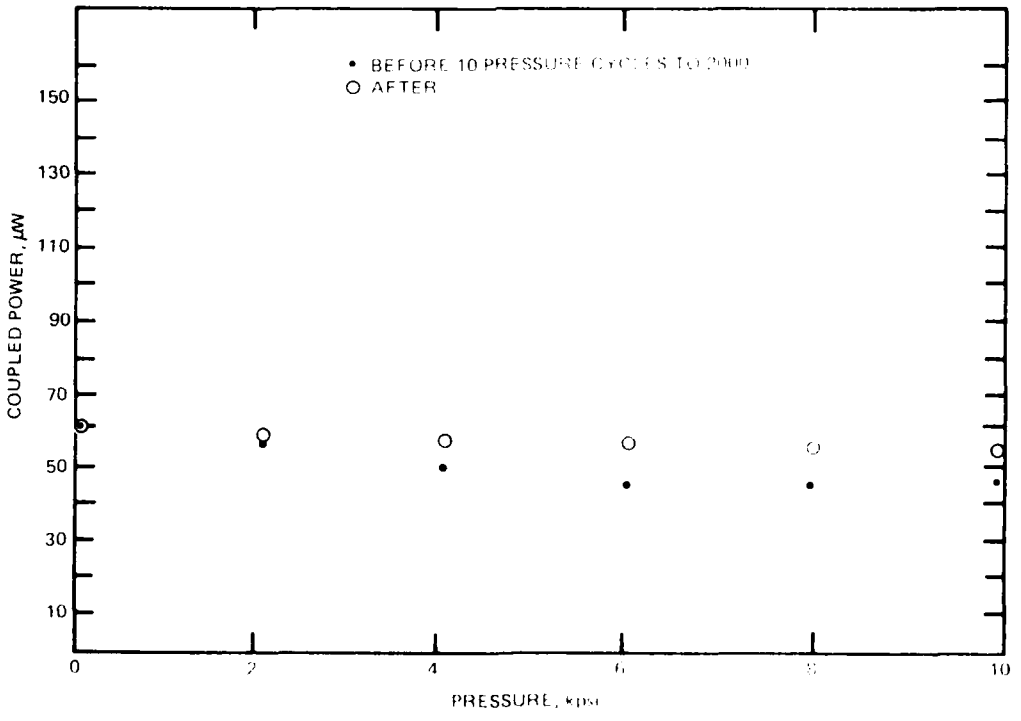

RCA C30123 100 mA FORWARD CURRENT

Figure 6. Coupled power vs pressure for the RCA C30123.

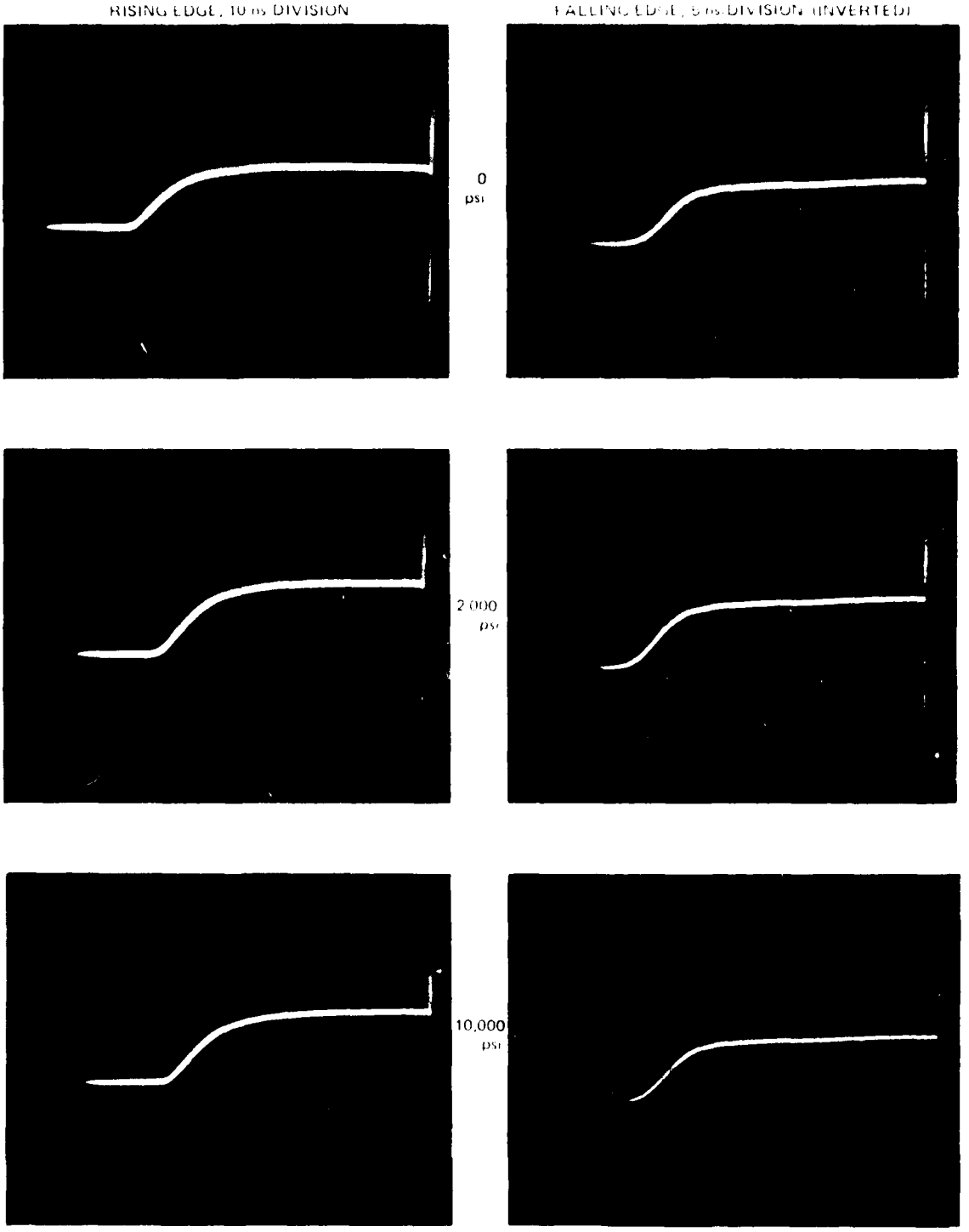
RISING EDGE, 10 ns DIVISION
FALLING EDGE, 5 ns DIVISION (INVERTED)
0
psi
2 000
psi
10,000
psi

Figure [illegible]

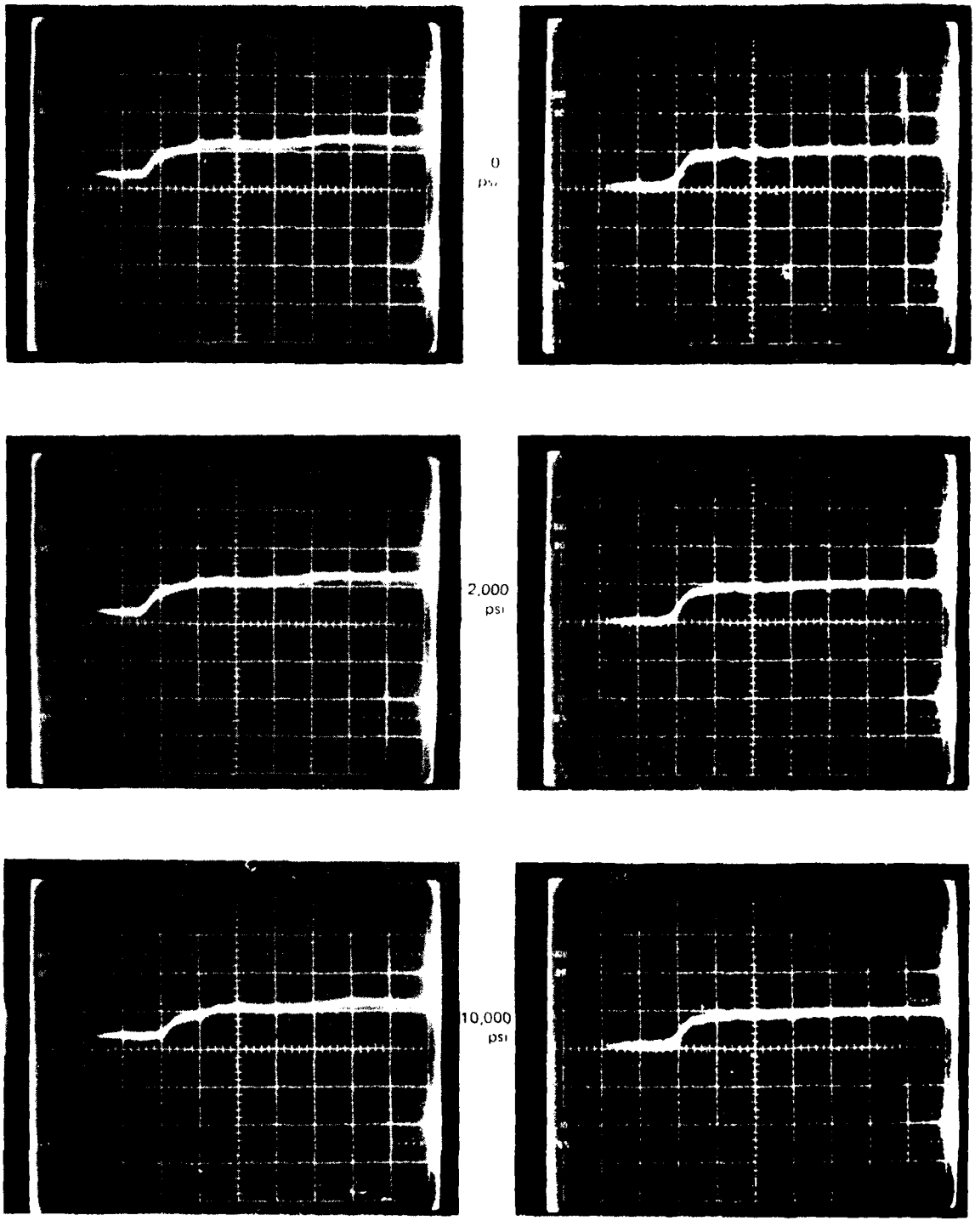
0
psi
2,000
psi
10,000
psi

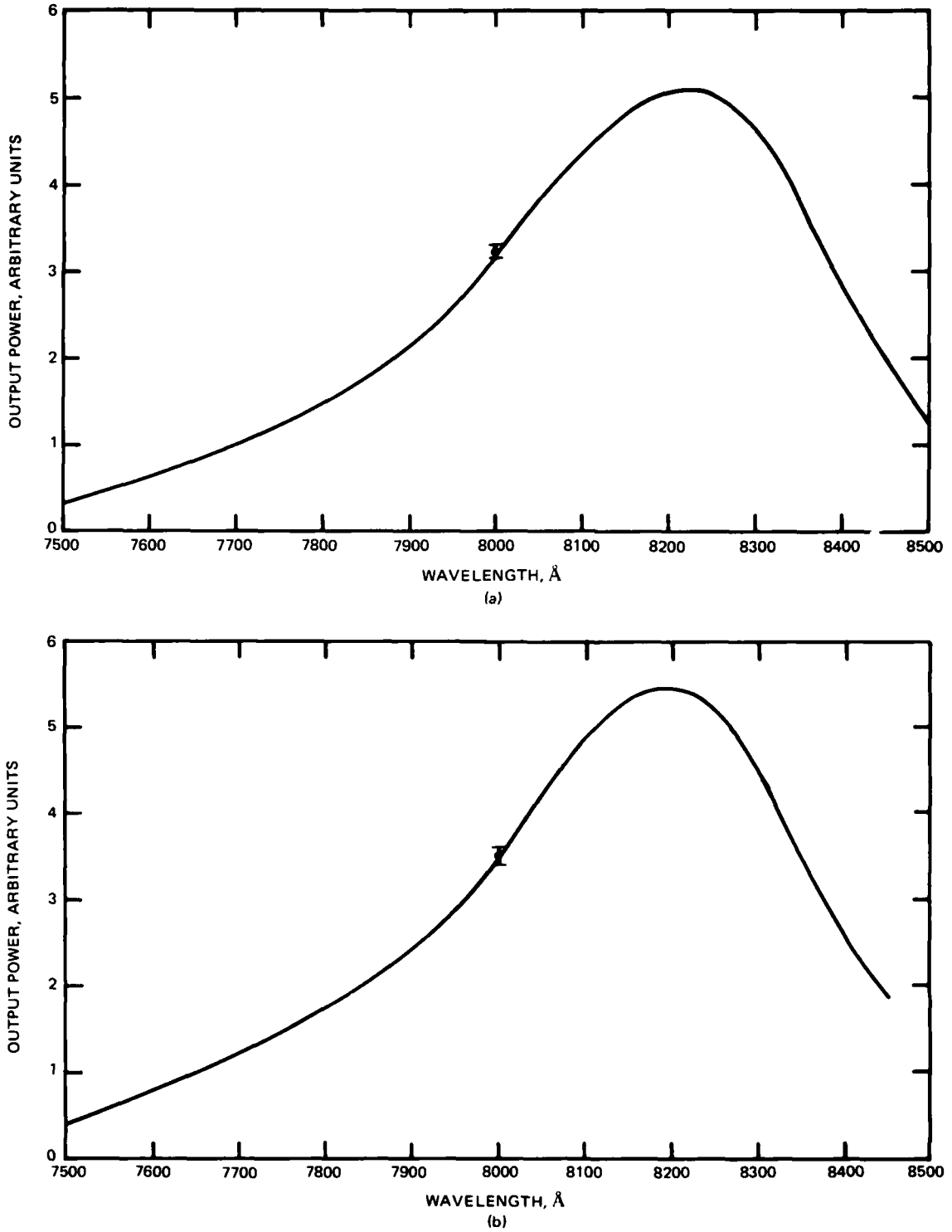

Figure 9. Relative output power vs wavelength at 0 psi (a) and 10 000 psi (b) for the Spectronics SE0352.

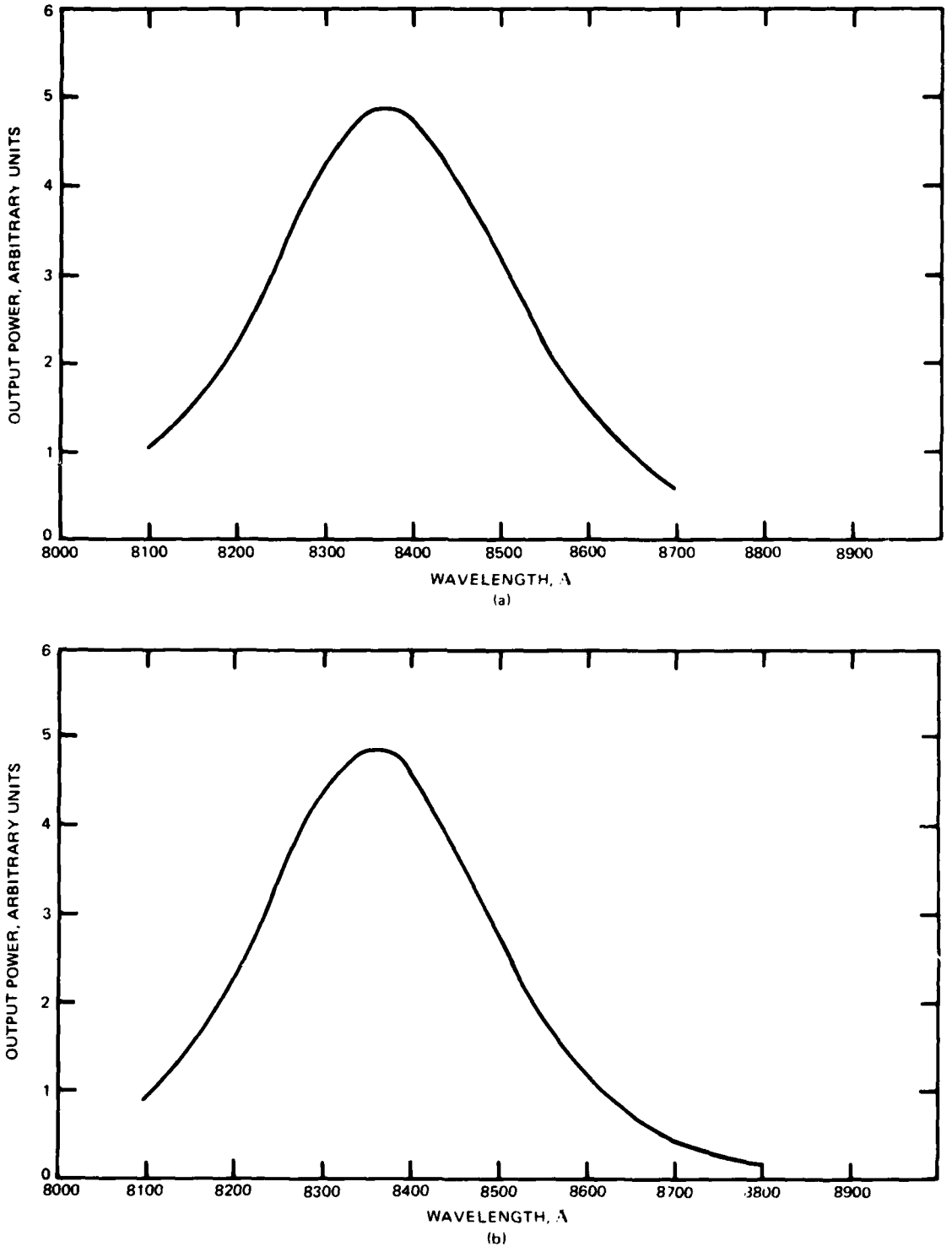

Figure 10. Relative output power vs wavelength at 0 psi (a) and 10 000 psi (b) for the RCA C 30123

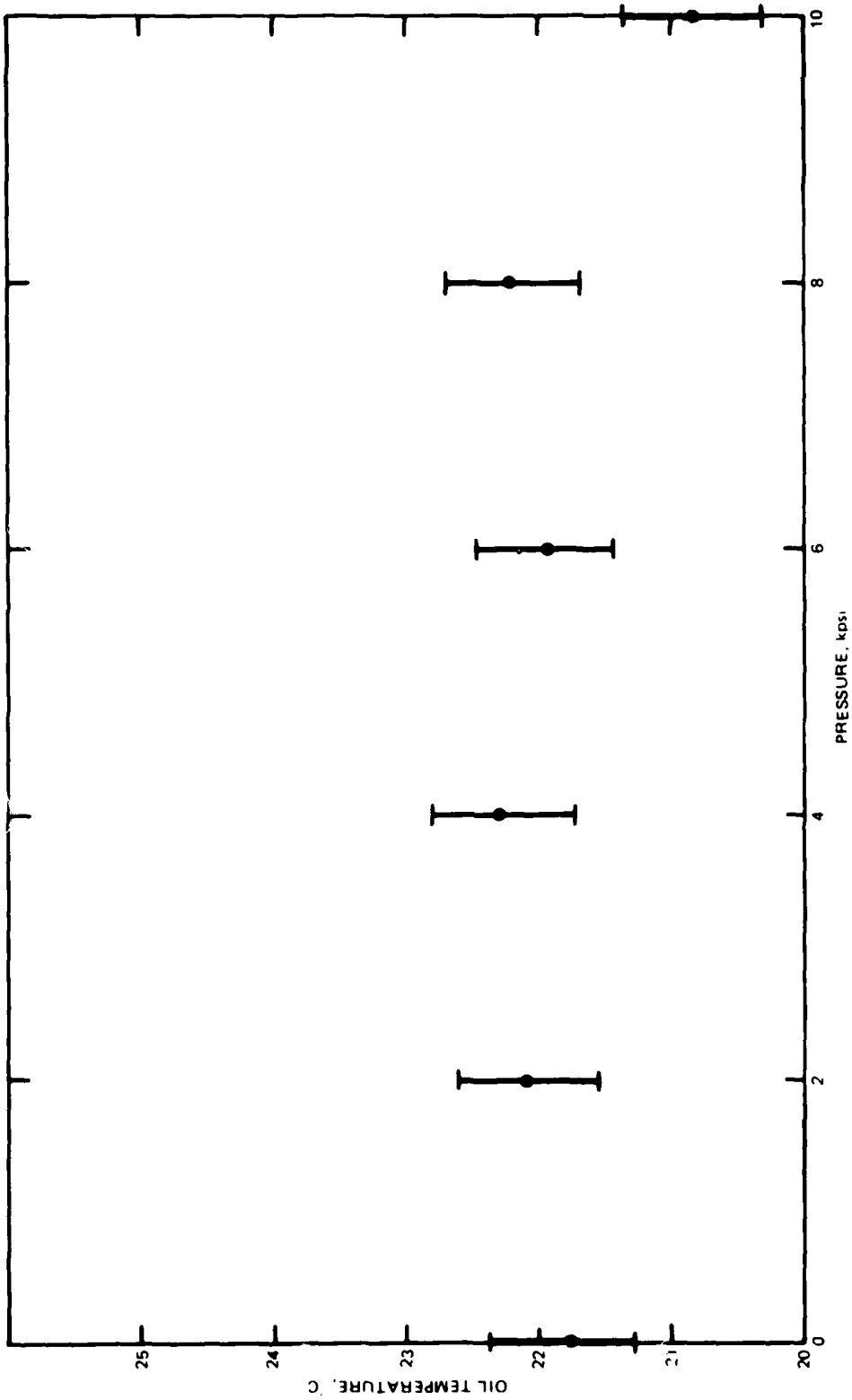

Figure 11 Hydraulic oil temperature measured at pressures up to 10 000 psi.

END

DATE
FILMED

5-81

DTIC